

Review

Electrochemical processing of spent nuclear fuels: An overview of oxide reduction in pyroprocessing technology

Eun-Young Choi^a, Sang Mun Jeong^{b,*}

^aKorea Atomic Energy Research Institute, Daedok-daero 989-111, Yuseong-gu, Daejeon 34057, Republic of Korea

^bDepartment of Chemical Engineering, Chungbuk National University, 1 Chungdae-ro, Seowon-Gu, Cheongju, Chungbuk 28644, Republic of Korea

Received 28 August 2015; accepted 30 October 2015

Available online 24 December 2015

Abstract

The electrochemical reduction process has been used to reduce spent oxide fuel to a metallic form using pyroprocessing technology for a closed fuel cycle in combination with a metal-fuel fast reactor. In the electrochemical reduction process, oxides fuels are loaded at the cathode basket in molten Li_2O – LiCl salt and electrochemically reduced to the metal form. Various approaches based on thermodynamic calculations and experimental studies have been used to understand the electrode reaction and efficiently treat spent fuels. The factors that affect the speed of the electrochemical reduction have been determined to optimize the process and scale-up the electrolysis cell. In addition, demonstrations of the integrated series of processes (electrorefining and salt distillation) with the electrochemical reduction have been conducted to realize the oxide fuel cycle. This overview provides insight into the current status of and issues related to the electrochemical processing of spent nuclear fuels.

© 2015 The Authors. Production and hosting by Elsevier B.V. on behalf of Chinese Materials Research Society. This is an open access article under the CC BY-NC-ND license (<http://creativecommons.org/licenses/by-nc-nd/4.0/>).

Keywords: Pyroprocessing; Electrochemical reduction; Electrorefining; Molten salt; Spent oxide fuel

1. Introduction

Nuclear energy is one of the global energy sources that can be used to meet the growing energy demand while avoiding CO_2 emissions into the environment. However, the accumulation of the spent fuel from nuclear power plants is a major hurdle in the use of nuclear energy. In Korea, about 700 t of spent fuel is produced from nuclear power plants every year. The total amount of spent fuel at the end of this century is anticipated to be more than 100,000 t [1]. Hence, recycling this spent fuel is part of the central focus of nuclear energy technology.

Pyroprocessing is a high-temperature electrochemical fuel processing technology for recycling the spent fuel into metal fuel for a nuclear fast reactor. In other words, pyroprocessing treats spent oxide fuels from light water reactors and produces metal fuels, which will

be irradiated in a nuclear fast reactor. The recycling of the fuel is expected to increase the uranium usage efficiency and decrease both the radiotoxicity and amount of the radioactive waste generated [2–9]. The process flow diagram of pyroprocessing in Korea consists of head-end processes, electrochemical processes (electrochemical reduction, electro-refining, and electro-winning), and waste treatment processes, as shown in Fig. 1 [10]. The purpose of the head-end processes, which consist of decladding, voloxidation, and oxide feed preparation, is to convert a spent fuel assembly into a suitable feed material that can be used in the electrochemical reduction process. In the voloxidation process, the dense oxide pellet discharged from the cladding hull is oxidized and pulverized to the powder form of U_3O_8 at a higher temperature than 500 °C under air atmosphere. The oxide feed with proper porosity and shape for the electrochemical processing is prepared with the voloxidized U_3O_8 powder.

Then, in the electrochemical reduction process (or oxide reduction process) based on a molten Li_2O – LiCl salt, the spent oxide fuel is reduced to supply metal feed to the electro-refining process. Additionally, high-heat-load fission products are dissolved into the molten Li_2O – LiCl salt, thus decreasing the heat load of the spent fuel.

*Corresponding author. Tel.: +82 43 261 3369; fax: +82 43 269 2370.

E-mail addresses: eychoi@kaeri.re.kr (E.-Y. Choi),
smjeong@chungbuk.ac.kr (S.M. Jeong).

Peer review under responsibility of Chinese Materials Research Society.

In electro-refining, pure uranium from the fuel is recovered in a molten LiCl–KCl eutectic salt, while uranium, transuranic elements, and rare earth elements are dissolved into the LiCl–KCl salt. The electrowinning process is used to recover the uranium and transuranic elements from the remaining salt after electrorefining [10–12].

This overview focuses on the electrochemical reduction process, which is the first step of the electrochemical fuel processing; it is organized as follows. First, the basic principles and related reports on the electrode reactions (cathode and anode) are reviewed. Second, the factors that affect the speed of the electrochemical reduction are discussed, which are required for the process optimization. Finally, a demonstration of the integrated series of processes (electrorefining and salt distillation) with the electrochemical reduction is introduced.

2. Electrode reactions of spent fuel in electrochemical reduction process

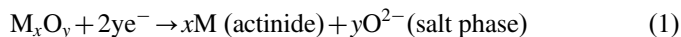
2.1. Cathode reactions

The electrochemical reduction process has been used to reduce the spent oxide fuel to the metallic form using pyroprocessing technology [13–16]. Conventionally, metallothemic reduction using lithium metal dissolved in a LiCl pool as a reductant (the so-called lithium reduction process) was used to reduce the spent oxide fuel, which had some drawbacks such as process complexity, solubility limit of the reactant and product, and handling of the chemically active lithium metal [17,18]. To tackle these problems, the electrochemical reduction method has been used for the reduction of the spent oxide fuel since a pioneer study by Chen et al. in the early 2000s [19]. This novel electrochemical reduction technology, so-called FFC-Cambridge process or electro-deoxidation process, made it possible to convert metal oxides directly into their parent metals by solid state electrolysis in a molten salt medium [20,21]. Although both the electrochemical reduction and the electro-deoxidation terms have been widely used in the literature [20,22,23], the electrochemical reduction has been preferred term in the nuclear field. Various advantages of electrochemical reduction have been reported for fuel processing [18,24,25]: (1) it involves no troublesome handling of lithium metal; (2) the concentration of oxide ions in the electrolyte medium can be maintained at a low level, which is thermodynamically favorable for the reduction of actinide and lanthanide elements; and (3) the process is much simpler and easier than the metallothemic reduction process.

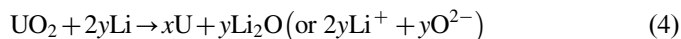
Extensive studies on the electrochemical reduction of uranium oxide, mixed oxide (MOX) fuel, and spent oxide fuels have been performed not only to measure the extent of the reduction of each element in the spent fuel or simulated fuel (SIMFUEL) [17,26–28], but also to understand the cathodic reaction pathways [13,24,29–31]. Although several molten salt systems have been tested for the reduction of oxide fuel [30–32], it seems that molten LiCl is the most promising option for the electrochemical reduction process for the following reasons: (1) the operating temperature can be lowered with LiCl salt because of its melting point, 605 °C

(e.g. melting point of CaCl₂, 772 °C); (2) a high current efficiency can be achieved with LiCl [30]; (3) O^{2–} has high solubility; and (4) in terms of its compatibility with the next electrochemical process, where the eutectic salt of LiCl–KCl is employed as the electrolyte, LiCl might be more suitable than any other salt.

In the electrochemical reduction process, oxides fuels are loaded at the cathode basket in molten LiCl, and some amount of Li₂O is added to speed up the reduction rate and prevent the anodic dissolution of the platinum anode by providing oxide ions to the salt [28]. The concentration of Li₂O added to LiCl is usually less than 3 wt% because a reaction between the produced uranium metal and Li₂O is not feasible even at such high concentrations. However, a concentration of 1 wt% of Li₂O is usually used by considering the corrosion resistance and degree of reduction in other oxides such as Pu₂O₃ and most of the rare earth oxides that occur in the spent fuel [33,34]. Based on the strategy of the head-end process, the spent oxide fuel can be loaded in various physical forms such as rod-cut, crushed particles, powder, and porous pellets [25,26,28,35,36], along with different oxidation states of uranium oxide, UO₂ or U₃O₈ [13,37]. The overall cathode reaction for the oxide fuel, mainly actinide oxides, is as follows:



Because uranium is a major element of the spent fuel, it is important to understand the electrochemical behavior of uranium oxide as a representative of actinide elements. When U₃O₈ is employed as a cathode material in the molten LiCl salt, various reaction intermediates appear during the electrochemical run [13,24]. Based on X-ray diffraction analysis, Jeong et al. reported that intermediates such as LiUO₃, U₄O₉, and UO₂ were formed at the beginning stage of the run (Fig. 1), and concluded that the reduction was started by the direct ionization mechanism lowering the oxidation states of the uranium and perovskite lithium uranate [13,38]. Then, the reduction of UO₂ was caused by two different reduction paths: the direct reduction and an electro-lithiothermic reduction assisted by the lithium metal produced in the fuel basket, as follows:



It is believed that both cathodic mechanisms occur because the decomposition voltages of the active actinide oxides are comparable to that of Li₂O [29,39].

While most of the previous studies have been conducted with unirradiated fuel, Idaho National Laboratory (INL, US) investigated the electrochemical reduction of spent oxide fuel in their hot cell facility [26,27]. These reports are valuable because they provide information on the reduction extent of each oxide in the spent fuel and the distribution of the fuel constituents between the salt and fuel phase (Table 1). Table 1 apparently suggests that 1) alkali and alkali earth metals such

as Cs, Ba, and Sr diffuse from the fuel and accumulate in the salt phase, as predicted by thermodynamic calculations [27]. 2) Actinides and noble metal oxides, except for zirconium, are readily reduced. 3) The rare earth and zirconium fission products are hardly converted to their metallic forms.

Although the electrochemical reduction of several rare earth oxides has been reported, most of the research is limited to low O^{2-} activity in the melt or co-reduction with the transition metal [40–44]. The thermodynamic calculation indicates that the activity of Li_2O should be kept much lower than 10^{-2} to obtain the rare earth metals from their oxides at 650 °C [33]. Thus, the unconverted rare earth oxides exist in the reduction product even after the electrochemical reduction process, where the Li_2O concentration is controlled to 1 wt%, as proven by INL's work [26]. Further studies on ways to increase the reduction of rare earth oxides are necessary because the unreduced oxides might chemically react with UCl_3 to form fine uranium oxide in the electrorefining step, which could contaminate the electrorefining salt [45].

2.2. Anode reactions

Carbon based materials have been widely employed as anode materials for molten salt electrolysis. In particular, graphite has been considered to be the first option because of its good electrical conductivity and low cost [34]. When carbon is used in the electro-deoxidation process (FFC Cambridge process), it becomes a consumable electrode because it is reactive to the O^{2-} ions dissolved out of the metal oxide and forms CO or CO_2 gas evolution [19,30,46]. In this case, the following reactions take place:



Feasibility studies of carbon anodes have been carried out based on thermodynamic calculations and electrochemical experiments for application to nuclear fuel processing using the Li_2O – $LiCl$ molten salt system [21,34,47,48]. The results of these studies indicated that a poor reduction yield and severe

carbon contamination of the metal oxide are obtained with an increase in the O^{2-} ion concentration in the molten salt due to the electrochemical decomposition of CO_3^{2-} ions, which are inevitably formed during the electrolysis. For this reason, an inert anode has been investigated for application to nuclear fuel processing.

Platinum has been employed as the anode material for the oxide reduction process of pyroprocessing. An earlier report

Table 1
Salt and fuel analysis results after electrochemical reduction of spent oxide fuel. Reprinted with permission from Ref. [23]. Copyright 2007 J. Nucl. Sci. Technol./Taylor & Francis Ltd. (www.tandfonline.com).

	Salt, pre-run (ppm)	Fuel, metal (wt%)	Fuel, oxide (wt%)	Salt, post-run (ppm)
Salt-soluble				
Cs	ND			111–119
Ba	40			140
Sr	15			65
Rb	ND			ND
Te	ND			75
Eu	ND			15
U/TRU				
U-total	50–82	98–99	1–2	2–5
Pu-total	1.9	93–96	4–7	0.3–0.4
Np-237	0.3	97–98	2–3	0.3–0.6
Am-241	ND	77–84	16–23	ND
Rare earths				
Nd	ND	36–43	57–64	ND
Ce	ND	40–49	51–60	ND
La	ND	ND	ND	ND
Pr	ND	38–47	53–62	ND
Sm	ND	27–33	67–73	ND
Y	ND	34–40	60–66	ND
Noble metals				
Zr	ND	ND–45	55–94	ND
Mo	ND	90–92	8–10	ND
Ru	ND	84–87	13–16	ND
Tc	ND	> 88	ND	ND
Pd	ND	> 75	ND	ND
Rh	ND	64–71	29–36	ND

ND=non-detectable (below minimum detection levels).

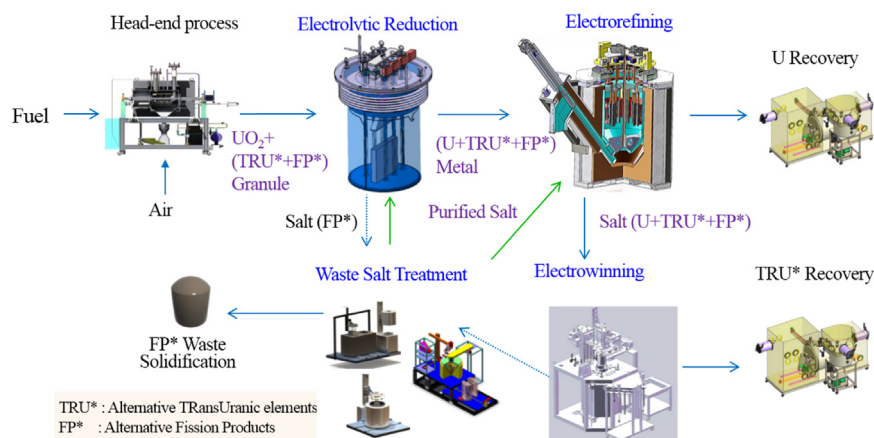


Fig. 1. Flow diagram of pyroprocessing in Korea.

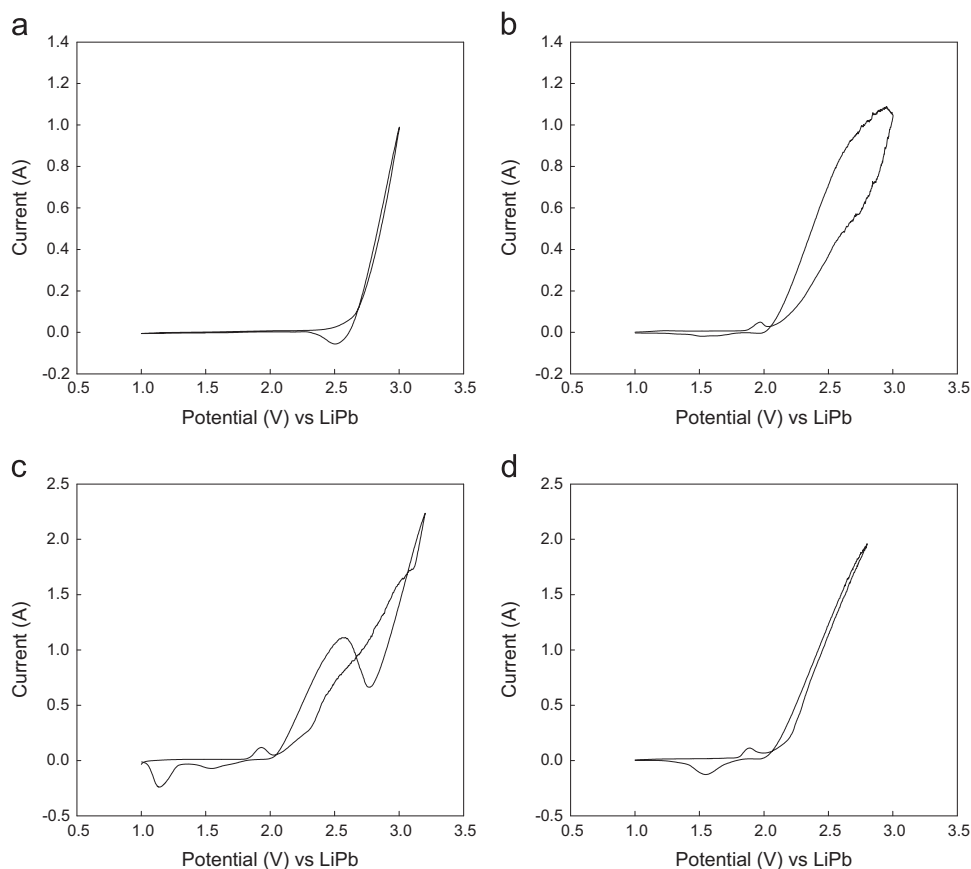
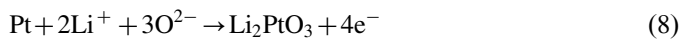


Fig. 2. Cyclic voltammograms of platinum wire at 650 °C. Electrolyte: (A) LiCl, (B) 0.5 wt% Li₂O/LiCl (scanning range: 1.0 to 3.2 V), (C) 0.5 wt% Li₂O/LiCl (scanning range: 1.0–3.0 V), and (D) 1 wt% Li₂O/LiCl. Scan rate: 100 mV/s; working electrode: Pt wire; counter electrode: Ni rod. Reprinted from Ref. [42], Copyright (2009), with permission from Elsevier.

regarded a Pt anode as an inert electrode when adding O^{2−} ions (Li₂O) to the LiCl melt because the main electrode reaction is the oxygen evolution [49]:



However, the current authors' group reported that a Pt anode could be corroded in two different ways, including the formation of Li₂PtO₃ at a higher Li₂O concentration and the direct dissolution of platinum at a lower O^{2−} ion concentration, as follows [46]:



They also reported that the direct dissolution is much more severe than the formation of Li₂PtO₃, and the optimal operation of the anode potential and O^{2−} ion concentration are key factors from the viewpoint of the loss of platinum. Cyclic voltammograms of a platinum anode with different concentrations of Li₂O are given in Fig. 2. Even though a platinum anode seems to be more suitable than graphite, it is very costly, and careful operation is necessary for application to molten salt electrolysis.

To overcome these problems, boron-doped diamond (BDD) has been tested as an alternative anode in an O^{2−} ion rich system [50–52]. A successful reduction of UO₂ was achieved

using a BDD electrode in a Li₂O–LiCl–KCl molten salt system [50]. However, the operating temperature was limited to a relatively low temperature (500 °C) because of its thermal stability [50,52]. In addition, the current density with the BDD electrode was much lower than that with platinum, which might have been caused by the lower operating temperature and a higher resistivity, that is, slow electrolysis kinetics. A recent report suggests that tungsten could be a potential anode material for the reduction of UO₂ in the Li₂O–LiCl system [52]. According to Merwin and Chidambaram's work, among the various metals tested, a tungsten anode exhibited sufficient stability at the required potential for oxide reduction in the Li₂O–LiCl melt, and such stability came from the formation of a lithium-intercalated oxide film on the tungsten surface [52]. However, their work was limited to a potentiodynamic polarization technique. Thus, a long-term feasibility test of a tungsten electrode seems to be necessary for application to nuclear fuel processing.

The anode system is one of the decisive factors in terms of the process stability and economics of a pyroprocessing technology. Even though a Pt anode is relatively stable compared to other electrode materials, it is believed that the commercialization of pyroprocessing technology can be promoted by the development of an alternative inert anode that is stable in a LiCl melt containing ~3 wt% Li₂O.

3. Process optimization of electrochemical reduction

Fig. 3 shows a schematic diagram of the typical cell used for electrochemical reduction. The electrolysis cell consists of a crucible, salt, and electrodes (cathode, anode, and reference). After LiCl containing Li₂O is loaded and melted in a crucible, the electrodes are immersed into the salt. The oxide fuel (metal oxides) is loaded and contained in a cathode basket with no loss into the salt. The Pt anode is usually surrounded by a shroud to offer a path for the O₂ gas produced on the anode surface.

The diffusion of O²⁻ ions from the inside of the oxide fuel to the bulk salt determines the reduction rate during electrolysis. This can be affected by 1) the accumulation of fission products in the salt [53], 2) characteristics of the oxide fuel in the cathode [35,54], 3) cathode containment material [55–57], 4) anode shroud [58], 5) electrode area [59], and 6) distance between the anode and cathode [60]. In the following section, we will review the reports on the factors that influence the electrochemical reduction rates in detail.

3.1. Accumulation of fission products in salt

Spent light water reactor (LWR) fuels consist of actinides (U, Pu, Np, Am, etc.), noble metals (Zr, Mo, Ru, Tc, Pd, Rh, Cd, Ag, etc.), rare earths (Nd, Ce, La, Pr, Sm, Y, Gd, Dy, etc.), and salt-soluble fission products (Cs, Ba, Sr, Rb, Te, I, and Eu). Because the salt-soluble fission products in the fuel are dissolved into the molten Li₂O–LiCl salt during the electrochemical reduction process, they are accumulated in the salt bath. Sakamura [53] investigated the effect of those fission products in the salt on the electrochemical reduction rate of UO₂. The electrochemical reduction rates were compared by conducting reduction tests of UO₂ in various LiCl salt baths containing 10–30 mol% of alkali and an alkaline–earth chloride such as KCl, CsCl, SrCl₂, or BaCl₂. It was observed that the presence of the alkali chlorides (KCl and CsCl) in the LiCl significantly prevented the electrochemical reduction reaction of UO₂. However, the addition of BaCl₂ to LiCl led to a slight decrease in the reduction rate of UO₂ compared to KCl or CsCl. Moreover, it was revealed that the SrCl₂ in LiCl hardly affected the electrochemical reduction reaction of UO₂. Such a change in the reduction rate by the accumulation of the salt-soluble fission products is due to a decrease in the solubility of O²⁻ ion in the salt [53,61].

These findings suggest that the accumulated fission products, Cs and Ba, gradually slow the speed of the electrochemical reduction when the LiCl salt is continuously used for numerous batches in a run. For example, if it is assumed that 1 kg of the fuel containing 0.25 wt% of Cs [62] is electrochemically reduced in 8 kg of LiCl, and all of the Cs is dissolved into the salt, 0.01 mol% of Cs in the LiCl is accumulated for every electrochemical reduction run. These results offer important information for determining the life time of the salt bath. If the Cs in the fuel is removed through head-end process, involving high-temperature voloxidation

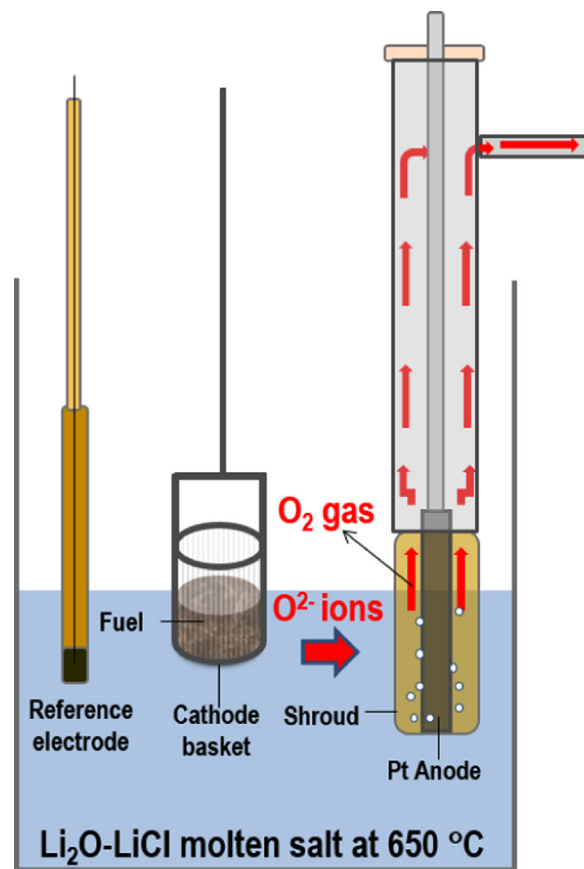


Fig. 3. Schematic diagram of electrochemical cell containing salt, cathode, anode, and reference electrode.

prior to the electrochemical reduction process, the life time of the salt bath will be significantly extended [63–65].

3.2. Effect of oxide fuel form in cathode

The transportation of O²⁻ ions in the fuel contained in the cathode basket is at least a few orders of magnitude slower than that in the bulk Li₂O–LiCl salt used for the electrochemical reduction [66,67]. Therefore, the diffusion rate of the O²⁻ ions in the fuel has a significant effect on the electrochemical reduction rate, which is determined by the characteristics of the fuel, such as its dimension and density. Many studies have shown through experiments [28,54,55,66–69] and simulations [70,71] that the transportation of O²⁻ ions in metal oxides with a low dimension and density is more advantageous than that in oxides with a high dimension and density. However, a powder-type fuel with a low dimension and density is not appropriate for the pyroprocessing of the electrochemical reduction process because a loss can occur during the process, making the nuclear accounting difficult. Hence, the current research group [35] systemically compared the electrochemical reduction rates of various UO₂ forms. The electrochemical reduction rates of eight UO₂ forms with different dimensions and densities (porous and dense forms) were compared. The electrolysis runs were conducted by loading the different UO₂ forms in the cathode basket and simultaneously performing electrolysis in 1.0 wt% Li₂O–LiCl. As reported by other groups

[54,66–71], it was confirmed that using UO_2 forms with a lower density and smaller size led to a faster electrochemical reduction rate. Interestingly, it was found that the size of the UO_2 had a more dominant effect on the reduction rate than the density [35]. This finding offers valuable information for designing the cathode basket because the use of a fuel with a small size and a high density would allow a reduction in the volume of the cathode basket. Moreover, the use of a small cathode basket would lead to a size reduction of the electrochemical reducer, which could have a significant effect on the cost of the process.

3.3. Cathode containment material

The cathode containment material is porous to allow the passage of the generated O^{2-} ions from the fuel to the bulk salt. However, its pore size should be smaller than the fuel particles to contain the fuel in the cathode basket with no loss into the salt. The current authors' group performed an electrochemical reduction using porous magnesia as a cathode basket to contain U_3O_8 powder [72–74]. Although the uranium metal was successfully achieved using it, even in a 20-kg U_3O_8 batch cell, the use of the porous magnesia was stopped because of its poor mechanical stability.

Herrmann et al. [55,57] investigated the electrochemical reduction behaviors in Li_2O – LiCl of different cathode containment materials, including a stainless steel (STS) wire mesh, sintered STS, and porous magnesia. The order of the Li_2O dissolution rates through the basket were the STS wire mesh > sintered STS > porous magnesia. Thus, they conducted the electrochemical reduction runs using the STS wire mesh and sintered STS. They found that the metal fraction from the reduction product in the STS wire mesh was 43–70%, with a value of 8–33% in the sintered STS basket. Moreover, the Li_2O concentration in the fuel contained in the STS wire mesh was 6.2–9.2 wt%, while that in the sintered STS basket was higher than its solubility in LiCl , 26–46 wt%. The results implied that the STS wire mesh was the most adequate among the tested cathode materials.

The pore size of the STS wire mesh should be properly selected to contain the fuel without its loss into the salt. The current authors' group tested four STS wire meshes with different numbers of layers (3 and 5 layers) and opening sizes for the electrochemical reduction process. The tested STS wire meshes are listed in Table 2 [56]. The opening sizes of the 325, 1400, and 2300 meshes used as the control layer were 40–43, 12–14, and 8–9 μm , respectively. Unexpectedly, the results of the tests using the various STS wire mesh baskets showed that the number of layers and the opening sizes did not have a significant influence on the electrochemical reduction performance. The UO_2 particles were successfully reduced to uranium metal with similar current densities and electrolysis times using the different types of STS wire mesh baskets. The main reason for this finding lies in the similar open area of the meshes (30–34%), which implies that this range of open area is sufficient for the diffusion of the O^{2-} ions. These results mean that the small opening size of a STS wire mesh basket used for

a fine fuel does not impede the transportation of the O^{2-} ions if it possesses a sufficient opening area.

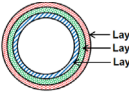

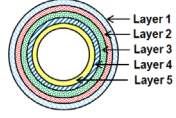
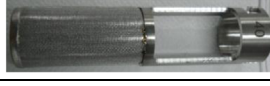


3.4. Anode shroud

As shown in the anode reaction (7), the electrochemical reduction process involves the generation of O_2 gas in a molten Li_2O – LiCl electrolyte, which produces a chemically aggressive environment that is too corrosive for the structure materials of the reducer [75,76]. Thus, the anode shroud controls the O_2 gas by offering a pathway to the outlet of the reduction equipment (Fig. 3). When a typical nonporous shroud made of a ceramic material is used, the O^{2-} ions are transported only through the open bottom of the anode shroud because it disturbs the transportation of the O^{2-} ions to the anode surface, which causes a decrease in the current density and an increase in the operation time of the process (Fig. 4a). Moreover, the ceramic shroud is fragile and inadequate for long-term use. Hence, the use of a porous shroud made of an STS wire mesh like the cathode basket was proposed [58]. Unlike a nonporous shroud, a porous shroud offers an open pathway for the O^{2-} ions through the pores in the side wall as well as its bottom (Fig. 4b). Porous shrouds made of ZrO_2 – MgO -coated and uncoated STS wire meshes with various opening sizes (20, 100, 300 meshes) were tested in electrochemical reduction runs. The results were compared with those of nonporous shrouds (MgO and MgO -stabilized ZrO_2). The observed current densities clearly showed that the current densities (0.76–0.79 A cm^{-2}) of the electrolysis runs using the porous anode shrouds were much higher than those (0.34–0.40 A cm^{-2}) of the runs using the nonporous shrouds. The ZrO_2 – MgO coating on the STS wire mesh was not stable because of the lithium metal in the Li_2O – LiCl . Interestingly, the electrolysis runs using the STS 20, 100, and 300 meshes showed similar current densities in spite of their different opening sizes, which implied that pores with a size of 40–43 μm are not an impediment to the transportation of O^{2-} ions. Moreover, the STS mesh shrouds, which were immersed in the Li_2O – LiCl electrolyte, were stable, without any damage or corrosion. This indicated that the O_2 gas liberated on the Pt anode surface did not leak through pores of this size. Recently, the current authors' group also succeeded in the electrochemical reduction of 1 kg of UO_2 using the STS wire mesh porous shroud [77] (Table 3).

3.5. Electrode area and distance between electrodes

It is well known that the current density of the electrochemical reduction process is affected by the electrode area [50,78]. Because the magnitude of the current is determined by the reactions, (1)–(5), a large area is advantageous to obtain a high current, which has a significant effect on the speed of the process. However, since the use of large electrodes requires a huge volume of the electrolyte salt, the determination of an optimal electrode surface area is needed, which is one of the key factors in designing an electrochemical reducer. The current authors' group [59] investigated the influence of the

Table 2
List of tested STS wire mesh cathode baskets. Reprinted from Ref. [53], Copyright (2014), with permission from Springer.

Mesh type	Mesh structure of the cathode basket	Type No.	1 st layer (Outer layer)	2 nd layer (Fine mesh-control layer)	3 rd layer	4 th layer	5 th layer	Pictures
3-layer		1	20 mesh	325 mesh	100 mesh	None	None	
5-layer		2	30 mesh	325 mesh	40 mesh	20 mesh	16 mesh	
		3		1400 mesh				
		4		2300 mesh				

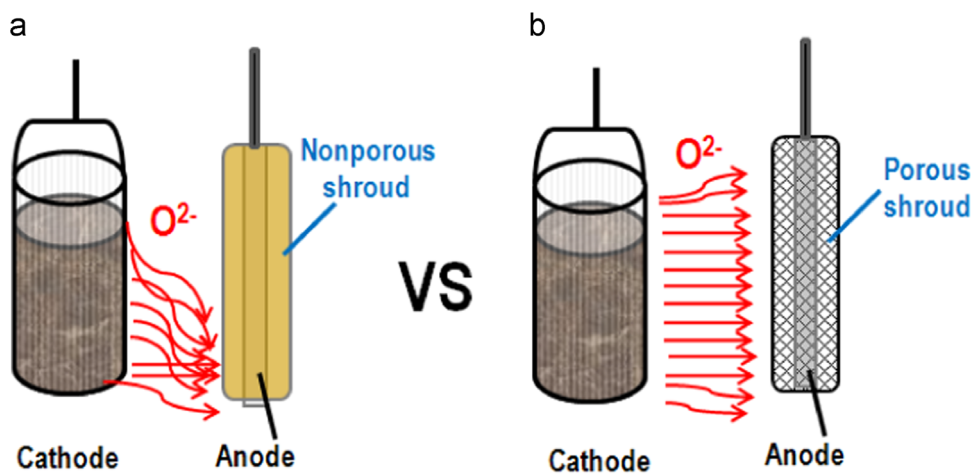


Fig. 4. Schematic diagram comparing nonporous and porous anode shrouds for electrochemical reduction process. Reprinted from Ref. [55], Copyright (2014), with permission from Elsevier.

cathode/anode surface area ratio on the current density of the bench-scale electrochemical reduction in $\text{Li}_2\text{O-LiCl}$ molten salt. It was observed that a low cathode/anode surface area ratio could lead to an increase in the current density during electrolysis, although this effect becomes insignificant if the cathode/anode surface area ratio falls below a minimum level. The electrochemical reduction of 17 kg of UO_2 was successfully performed using equipment with a cathode/anode surface area ratio of 2.6. However, the determination of an optimal cathode/anode surface area ratio that can be universally applied to other electrochemical reducers is still controversial because other design factors also affect the current density.

In addition, it was reported that the electrochemical reduction is influenced by the distance between the cathode and anode [60]. Different anode-to-cathode distances (1.3, 2.3, 3.2, 3.7, and 5.8 cm) were tested to select the optimal electrolysis cell configuration. The experimental results showed that the



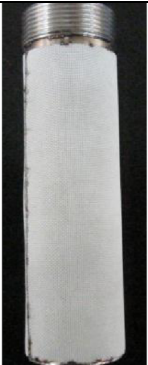



current increases as the anode-to-cathode distance decreases during electrolysis using a constant voltage. These findings imply that a short anode-to-cathode distance is advantageous to accelerate the electrochemical reduction process, which is a very important factor when designing a reducer.

4. Integrated series of pyroprocessing steps

INL demonstrated an integrated series of electrochemical reduction and electrorefining processes using spent light water reactor fuel in a hot cell [62]. The spent oxide fuel for the feed of the electrochemical reduction was prepared by separating it from its cladding, sectioning, crushing, and sieving. In a bench-scale (~60 g) electrochemical reduction experiment, the spent oxide fuel was successfully reduced to metal, and all of the metal fractions of uranium, plutonium, and neptunium in the reduction product were higher than 97%. It was

Table 3

List of six types of tested anode shrouds. Reprinted from Ref. [55], Copyright (2014), with permission from Elsevier.

Nonporous shroud		Porous shroud			
Dense MgO	MgO (3 wt%) -ZrO ₂	MgO (3 wt%) -ZrO ₂ coated STS 40 mesh	STS 20 mesh	STS 100 mesh	STS 300 mesh
					

confirmed that the fission products such as Cs, Sr, and Ba were dissolved and accumulated in the molten Li₂O–LiCl salt. However, only 71–82% of the fission products were dissolved from the fuel, implying that the partial fission products did not dissolve into the salt or remained in the salt contained within the fuel pellet. The prepared reduction product was used as a feed for the electrorefining after it was loaded into an anode basket. During the electrorefining process in LiCl–KCl–UCl₃ at 500 °C, uranium, transuranic elements, and other fission products were dissolved at the anode, but only uranium metal was deposited at the STS cathode.

The Central Research Institute of the Electric Power Industry (CRIEPI, Japan) also performed an integrated series of electrochemical reduction and electrorefining processes in bench-scale (~100 g) experiments using unirradiated fuel [79]. Unlike INL's work, porous UO₂ pellets were used as the feed of the electrochemical reduction. In the head-end process, the porous UO₂ pellets were prepared from spent fuel by decladding, voloxidation, pelletizing, and sintering; the starting material (UO₂ dense pellets) was oxidized to U₃O₈ powder at 1000 °C in air. Then, cylindrical porous pellets were produced by compacting U₃O₈ powder under high pressure and sintering at 1700 °C. During the head-end process, some volatile fission products such as cesium and tellurium were separated from the fuel, which prevented their accumulation in the electrochemical reduction salt and helped maintain its efficiency.

The Korea Atomic Energy Research Institute (KAERI) conducted a series of pyroprocessing steps using a single STS wire mesh basket as the fuel containment material to minimize fuel loss [80]. This single STS wire mesh basket was

used in a series of processes that included electrochemical reduction, LiCl distillation, electrorefining, LiCl–KCl distillation, and finally a second electrochemical reduction and subsequent LiCl distillation step (Fig. 5). The salt distillation processes were carried out at 850 °C under a vacuum condition to remove the salt contained within the fuel pellet and prevent a change in the salt composition in the subsequent process. It was demonstrated that the entire cycle of processes could be successfully conducted with a single STS wire mesh basket without loading or unloading the fuel. However, an intermetallic layer of uranium (from the fuel)–iron (from the STS basket) was observed on the cross-section of the STS basket wall as a result of a eutectic reaction between them. The influence of this intermetallic layer on the lifetime of the basket is being studied.

5. Conclusions

An electrochemical processing technology for spent nuclear fuel, the so-called pyroprocessing, has been developed to meet the growing energy demand and to prevent CO₂ emissions into the environment at the same time. The electrochemical reduction process has been employed to reduce the spent oxide fuel to a metallic form using pyroprocessing technology for a closed fuel cycle in combination with a metal fuel fast reactor. Many studies have been successfully conducted to understand the fundamentals of the electrochemical reduction of various fuels and to optimize the electrolysis cell for handling the spent nuclear fuel. Thus, impressive progress in the oxide reduction process used to treat spent fuel has been made by the research activities of several nuclear research

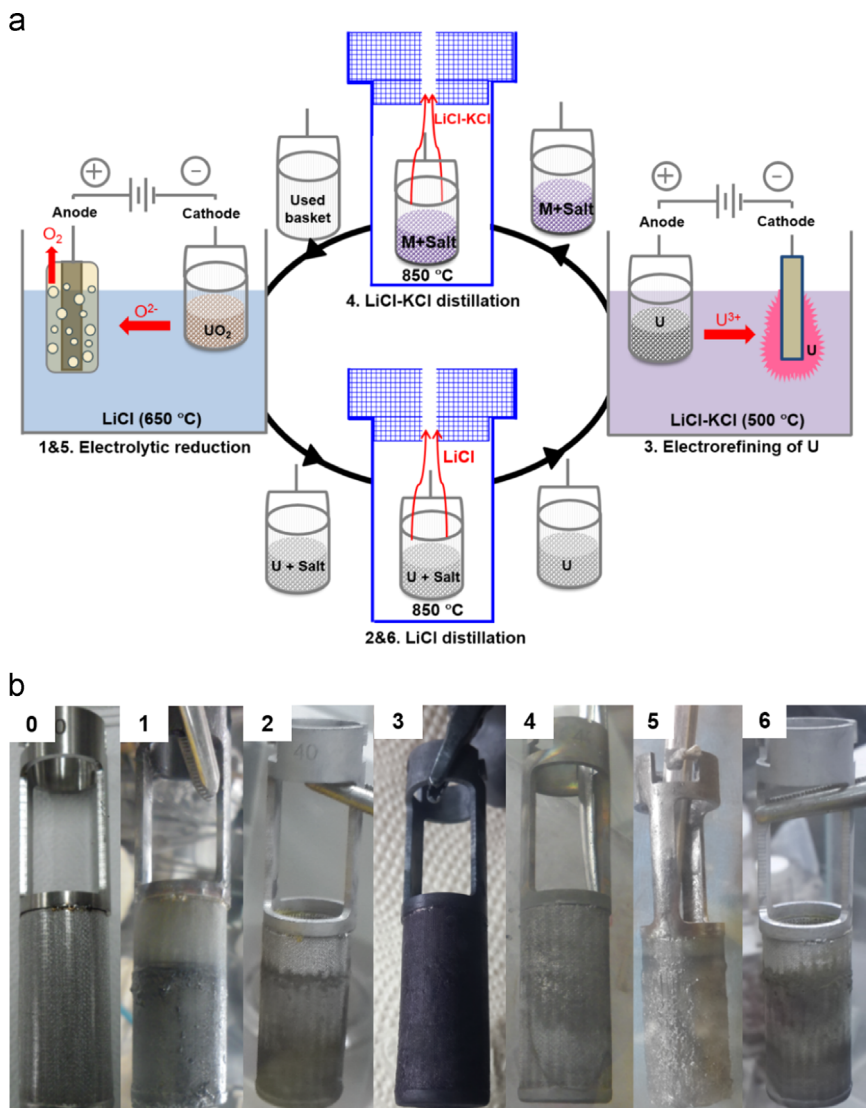


Fig. 5. (a) Schematic diagram of processes performed using STS wire mesh basket: 1) electrolytic reduction of UO_2 , 2) LiCl distillation of reduction product, 3) electrorefining of U , 4) LiCl-KCl distillation, 5) second electrolytic reduction of fresh UO_2 in used basket, and 6) second LiCl distillation of reduction product. (b) Photographs of baskets 0) before use and after 1–6) the processes with the corresponding numbers. Reprinted from Ref. [77], Copyright (2015), with permission from Elsevier.

institutes such as KAERI, CRIEPI, INL, Argonne National Laboratory (ANL), and the Indira Gandhi Centre for Atomic Research (IGCAR). Based on the results of these fundamental studies, the technical interest has now turned toward the development of an engineering-scale electrolysis cell and integrated operation involving oxide reduction and electrorefining processes.

KAERI is running the PRIDE Facility, which is an engineering scale (10 t/year in capacity) facility operated remotely using manipulators in an Ar environment, to demonstrate the integrity of all of the unit processes of pyroprocessing. Nevertheless, many challenges need to be tackled to commercialize the electrochemical fuel processing technology to solve the issue of spent fuel accumulation. This technology can be further developed by a technical convergence between chemists, material scientists, chemical, mechanical, and nuclear engineers.

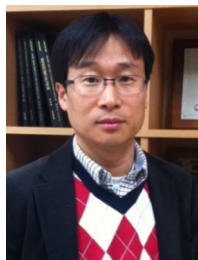
Acknowledgment

This work was supported by a National Research Foundation of Korea (NRF) Grant funded by the Korea Government (MISP) (2015M2B2A9030532; 2012M2A8A5025697).

References

- [1] Y.I. Kim, S.G. Hong, D. Hahn, *Nucl. Eng. Technol.* 40 (2008) 517–526.
- [2] J.J. Laidler, J.E. Battles, W.E. Miller, J.P. Ackerman, E.L. Carls, *Prog. Nucl. Energy* 31 (1997) 131–140.
- [3] J.P. Ackerman, T.R. Johnson, L.S.H. Chow, E.L. Carls, W.H. Hannum, J.J. Laidler, *Prog. Nucl. Energy* 31 (1997) 141–154.
- [4] R.W. Benedict, H.F. McFarlane, *Radwaste Mag.* 5 (1998) 23.
- [5] T. Inoue, L. Koch, *Nucl. Eng. Technol.* 40 (2008) 183–190.
- [6] T. Inoue, T. Koyama, Y. Arai, *Energy Procedia* 7 (2011) 405–413.
- [7] K.M. Goff, J.C. Wass, K.C. Marsden, G.M. Teske, *Nucl. Eng. Technol.* 43 (2011) 335–342.

- [8] K. Nagarajan, B.P. Reddy, S. Ghosh, G. Ravisankar, K.S. Mohandas, U.K. Mudali, K.V.G. Kuty, K.V.K. Viswanathan, C.A. Babu, P. Kalyanasundaram, P.R.V. Rao, B. Raj, *Energy Procedia* 7 (2011) 431–436.
- [9] T. Koyama, Y. Sakamura, M. Iizuka, T. Kato, T. Murakami, J.-P. Glatz, *Procedia Chem.* 7 (2012) 772–778.
- [10] H. Lee, G.I. Park, J.W. Lee, K.H. Kang, J.M. Hur, J.G. Kim, S. Paek, I. T. Kim, I.J. Cho, *Sci. Technol. Nucl. Install.* 2013 (2013) 343492.
- [11] K.C. Song, H. Lee, J.M. Hur, J.G. Kim, D.H. Ahn, Y.Z. Cho, *Nucl. Eng. Technol.* 42 (2010) 131–144.
- [12] H. Lee, J.M. Hur, J.G. Kim, D.H. Ahn, Y.Z. Cho, S.W. Paek, *Energy Procedia* 7 (2011) 391–395.
- [13] S.M. Jeong, H.S. Shin, S.S. Hong, J.M. Hur, J.B. Do, H.S. Lee, *Electrochim. Acta* 55 (2010) 1749–1755.
- [14] J.L. Willit, W.E. Miller, J.E. Battles, *J. Nucl. Mater.* 195 (1992) 229–249.
- [15] T. Usami, M. Kurata, T. Inoue, H.E. Sims, S.A. Beetham, J.A. Jenkins, *J. Nucl. Mater.* 300 (2002) 15–26.
- [16] J.H. Yoo, C.S. Seo, E.H. Kim, H.S. Lee, *Nucl. Eng. Technol.* 40 (2008) 581–592.
- [17] S.M. Jeong, B.H. Park, J.M. Hur, C.S. Seo, H.S. Lee, K.C. Song, *Nucl. Eng. Technol.* 42 (2010) 183–192.
- [18] M. Iizuka, Y. Sakamura, T. Inoue, *J. Nucl. Mater.* 359 (2006) 102–113.
- [19] G.Z. Chen, D.J. Fray, T.W. Farthing, *Nature* 407 (2000) 361–364.
- [20] C. Schwandt, D.T.L. Alexander, D.J. Fray, *Electrochim. Acta* 54 (2009) 3819–3829.
- [21] T. Biju Joseph, N. Sanil, K.S. Mohandas, K. Nagarajan, *J. Electrochem. Soc.* 162 (2015) E51–E58.
- [22] T. Wu, X. Jin, W. Xiao, X. Hu, D. Wang, G.Z. Chen, *Chem. Mater.* 19 (2007) 153–160.
- [23] K. Jiang, X. Hu, M. Ma, D. Wang, G. Qiu, X. Jin, G.Z. Chen, *Angew. Chem. Int. Ed.* 45 (2006) 428–432.
- [24] B.H. Park, I.W. Lee, C.S. Seo, *Chem. Eng. Sci.* 63 (2008) 3485–3492.
- [25] S.M. Jeong, J.M. Hur, S.S. Hong, D.S. Kang, M.S. Choung, C.S. Seo, J.S. Yoon, S.W. Park, *Nucl. Technol.* 162 (2008) 184–191.
- [26] S.D. Herrmann, S.X. Li, M.F. Simpson, *Sep. Sci. Technol.* 41 (2006) 1965–1983.
- [27] S.D. Herrmann, S.X. Li, M.F. Simpson, *J. Nucl. Sci. Technol.* 44 (2007) 361–367.
- [28] E.Y. Choi, J.W. Lee, J.J. Park, J.M. Hur, J.K. Kim, K.Y. Jung, S.M. Jeong, *Chem. Eng. J.* 514 (2012) 207–208.
- [29] J.M. Hur, S.M. Jeong, H. Lee, *Electrochem. Commun.* 12 (2010) 706–709.
- [30] Y. Sakamura, M. Kurata, T. Inoue, *J. Electrochem. Soc.* 153 (2006) D31–D39.
- [31] D.S.M. Vishnu, N. Sanil, G. Panneerselvam, R. Sudha, K.S. Mohandas, K. Nagarajan, *J. Electrochem. Soc.* 160 (2013) D394–D402.
- [32] D.S.M. Vishnu, N. Sanil, G. Panneerselvam, S.K. Mahato, K.V. Soja, K.S. Mohandas, K. Nagarajan, *J. Electrochem. Soc.* 160 (2013) D583–D592.
- [33] B.H. Park, S.B. Park, S.M. Jeong, C.S. Seo, S.W. Park, *J. Radioanal. Nucl. Chem.* 270 (2006) 575–583.
- [34] K.S. Mohandas, *Trans. Inst. Min. Metall. C* 122 (2013) 195–212.
- [35] E.Y. Choi, J.K. Kim, H.S. Im, I.K. Choi, S.H. Na, J.W. Lee, S.M. Jeong, J.M. Hur, *J. Nucl. Mater.* 437 (2013) 178–187.
- [36] J.M. Hur, S.S. Hong, H. Lee, *J. Radioanal. Nucl. Chem.* 295 (2013) 851–854.
- [37] Y. Sakamura, T. Omori, T. Inoue, *Nucl. Technol.* 162 (2008) 169–178.
- [38] A.M. Abdelkader, K.T. Kilby, A. Cox, D.J. Fray, *Chem. Rev.* 113 (2013) 2863–2886.
- [39] W. Xiao, D. Wang, *Chem. Soc. Rev.* 43 (2014) 3215–3228.
- [40] A.M. Abdelkader, D.J.S. Hyslop, A. Cox, D.J. Fray, *J. Mater. Chem.* 20 (2010) 6039–6049.
- [41] H.S. Ji, H.Y. Ryu, E.Y. Choi, S.W. Cho, M.F. Simpson, S.M. Jeong, *J. Ind. Eng. Chem.* 24 (2015) 259.
- [42] D. Wang, G. Qiu, X. Jin, X. Hu, G.Z. Chen, *Angew. Chem. Int. Ed.* 45 (2006) 2384–2388.
- [43] G. Qiu, D. Wang, M. Ma, X. Jin, G.Z. Chen, *J. Electroanal. Chem.* 589 (2005) 139–147.
- [44] Y. Zhang, H. Yin, S. Zhang, D. Tang, Z. Yuan, T. Yan, W. Zheng, D. Wang, *J. Rare Earths* 30 (2012) 923–927.
- [45] Y.H. Kang, S.C. Hwang, H.S. Lee, E.H. Kim, S.W. Park, J.H. Lee, *J. Mater. Process. Technol.* 209 (2009) 5008–5013.
- [46] S.M. Jeong, H.S. Shin, S.H. Cho, J.M. Hur, H.S. Lee, *Electrochim. Acta* 54 (2009) 6335–6340.
- [47] H.Y. Ryu, S.M. Jeong, Y.C. Kang, J.G. Kim, *Asian J. Chem.* 25 (2013) 7019–7022.
- [48] J.M. Hur, J.S. Cha, E.Y. Choi, *ECS Electrochem. Lett.* 3 (2014) E5–E7.
- [49] K.V. Gourishankar, L. Redey, M. Williamson, in: W. Schneider (Ed.), *Light Metals, The Minerals, Metals & Materials Society*, 2002, pp. 1075–1082.
- [50] W. Park, J.K. Kim, J.M. Hur, E.Y. Choi, H.S. Im, S.S. Hong, *J. Nucl. Mater.* 432 (2013) 175–181.
- [51] Y. Kado, T. Goto, R. Hagiwara, *Diam. Relat. Mater.* 18 (2009) 1186–1190.
- [52] A. Mervin, D. Chidambaram, *Metall. Mater. Trans. A* 46 (2015) 536–544.
- [53] Y. Sakamura, *J. Nucl. Mater.* 412 (2011) 177–183.
- [54] E.J. Karell, K.V. Gourishankar, J.L. Smith, L.S. Chow, L. Redey, *Nucl. Technol.* 136 (2001) 342–353.
- [55] S.D. Herrmann, S.X. Li, B.E. Serrano-Rodriguez, in: *Proc. Global, Paris, France*, 2009, p. 9059.
- [56] E.Y. Choi, C.Y. Won, D.S. Kang, S.W. Kim, J.S. Cha, S.J. Lee, W. Park, H.S. Im, J.M. Hur, *J. Radioanal. Nucl. Chem.* 304 (2015) 535–546.
- [57] S.D. Herrmann, S.X. Li, D.A. Sell, B.R. Westphal, in: *Proc. Global, Boise, Idaho*, 2007, pp. 758.
- [58] E.Y. Choi, C.Y. Won, J.S. Cha, W. Park, H.S. Im, S.S. Hong, J.M. Hur, *J. Nucl. Mater.* 444 (2014) 261–269.
- [59] E.Y. Choi, J.M. Hur, I.K. Choi, S.G. Kwon, D.S. Kang, S.S. Hong, H.S. Shin, M.A. Yoo, S.M. Jeong, *J. Nucl. Mater.* 418 (2011) 87–92.
- [60] E.Y. Choi, H.S. Im, J.M. Hur, *J. Korean Electrochem. Soc.* 16 (2013) 138–144.
- [61] Y. Sakamura, *J. Electrochem. Soc.* 157 (2010) E135–E139.
- [62] S.D. Herrmann, S.X. Li, *Nucl. Technol.* 171 (2010) 247–265.
- [63] B.R. Westphal, K.J. Bateman, C.D. Morgan, J.F. Berg, P.J. Crane, D. G. Cummings, J.J. Giglio, M.W. Huntley, R.P. Lind, D.A. Sell, *Nucl. Technol.* 162 (2008) 153–157.
- [64] K.C. Song, G.I. Park, J.W. Lee, J.J. Park, M.S. Yang, *Nucl. Technol.* 162 (2008) 158–168.
- [65] H. Lee, G.I. Park, K.H. Kang, J.M. Hur, J.G. Kim, D.H. Ahn, Y.Z. Cho, E.H. Kim, *Nucl. Eng. Technol.* 43 (2011) 317–328.
- [66] E. Gordo, G.Z. Chen, D.J. Fray, *Electrochim. Acta* 49 (2004) 2195–2208.
- [67] S. Phongikaroon, S.D. Herrmann, M.F. Simpson, *Nucl. Technol.* 174 (2011) 85–93.
- [68] P. Kar, J.W. Evans, *Electrochim. Acta* 53 (2008) 5260–5265.
- [69] P. Kar, J.W. Evans, *Electrochim. Acta* 54 (2008) 835–843.
- [70] E. Ergul, I. Karakaya, M. Erdogan, *J. Alloy. Compd.* 509 (2011) 899.
- [71] K.S. Mohandas, D.J. Fray, *Metall. Mater. Trans. B* 40 (2009) 685–699.
- [72] J.M. Hur, C.S. Seo, S.S. Hong, D.S. Kang, S.W. Park, *React. Kinet. Catal. Lett.* 80 (2003) 217–222.
- [73] S.M. Jeong, S.B. Park, S.S. Hong, C.S. Seo, S.W. Park, *J. Radioanal. Nucl. Chem.* 268 (2006) 349–356.
- [74] C.S. Seo, S.B. Park, B.H. Park, K.J. Jung, S.W. Park, S.H. Kim, *J. Nucl. Sci. Technol.* 43 (2006) 587–595.
- [75] J.E. Indacochea, J.L. Smith, K.R. Litko, E.J. Karell, A.G. Raraz, *Oxid. Met.* 55 (2001) 1–16.
- [76] S.H. Cho, S.B. Park, D.S. Kang, M.S. Jeong, H. Park, J.M. Hur, H.S. Lee, *J. Nucl. Mater.* 399 (2010) 212–218.
- [77] E.Y. Choi, J. Lee, M.K. Jeon, S.K. Lee, S.W. Kim, S.C. Jeon, J.H. Lee, J.M. Hur, *Accepted manuscript, Submitted to J. Korean Electrochem. Soc. (in Korean)*.
- [78] H. Chen, X. Jin, L. Yu, G.Z. Chen, *J. Solid State Electrochem.* 18 (2014) 3317–3325.
- [79] Y. Sakamura, T. Omori, *Nucl. Tech.* 171 (2010) 266–275.
- [80] E.Y. Choi, C.Y. Won, S.-J. Lee, D.-S. Kang, S.-W. Kim, J.-S. Cha, W. Park, H.S. Im, J.-M. Hur, *Ann. Nucl. Tech.* 76 (2015) 305–314.



Sang Mun Jeong is a professor in the Department of chemical Engineering, Chungbuk National University and a director of the Korean Institute of Chemical Engineers. He obtained his Ph.D. degree in Chemical Engineering from Korea Advanced Institute of Science and Technology (KAIST) in 1999. He worked previously at CPE Lyon (France), University of Nottingham (UK), University of Utah (US), LG Chemical and Korea Atomic Energy Research Institute (KAERI). He has published over

70 articles on chemical and electrochemical reactions for application to energy, environment and materials and is cited as the inventor on over 20 patents.